The effects of increasing FAME biodiesel content on combustion characteristics and HC emissions in high-EGR low temperature combustion

Oluwasujibomi Sogbesan[a], Colin P. Garner[a], Martin H. Davy[b]

[a] *Wolfson School of Mechanical, Electrical and Manufacturing Engineering, Loughborough University, UK*
[b] *Department of Engineering Science, University of Oxford, UK*

Abstract

An experimental study was performed on a single-cylinder high-speed direct-injection diesel research engine to determine the effects of increasing biodiesel content on the combustion characteristics and HC emissions during high-EGR low temperature combustion operation. Two test points, a moderately dilute low-load condition and a high-EGR medium-load condition, were examined at a constant speed of 1500 rpm with a fixed input fuel energy content and start of injection timing.

The results show the two operating conditions to have very different sensitivities to the fuel's biodiesel content and, as a result, to demonstrate contrasting behaviour with respect to the variation of HC emissions with blend composition. For the low load, medium dilution case, ignition delay, combustion phasing and combustion duration are essentially independent of biofuel content while HC emissions are reduced with respect to the base diesel. For the high-EGR, medium load condition, ignition delay is reduced and combustion phasing advances with increasing levels of biofuel content. HC emissions increase with increasing biofuel content. Crank-angle aligned HC measure-

ments indicate the significance of the piston/wall crevice volume as an HC source in high-EGR LTC.

Keywords: LTC, PPCI, Biodiesel, FAME, HC emissions

1. Introduction

The use of biodiesel as a renewable energy source to supplement petroleum diesel has come about via legislative constraints that are aimed at managing fossil fuel energy consumption. In Europe for example, current EU Directive 2009/28/EC mandates that a minimum of 10 % of transportation fuel should be from renewable sources [1], while Directive 2018/2001/EC sets a future target of a minimum of 14 % renewable sourced fuel by 2030 in every Member State [2]. This has stimulated research effort aimed at understanding the effects of increasing biodiesel content on compression ignition (CI) engine combustion behaviour.

For conventional diesel combustion regimes, a fairly disparate range of results have been observed for biodiesels (typically blends of petroleum diesel and biodiesel produced by the transesterification of vegetable oils or animal fats)—partly due to non-uniformity of feedstocks, relative volume contents, engine parameters and operating conditions. Nevertheless, there is now widespread consensus regarding the impact of biodiesel on: fuel conversion efficiency, where no significant difference is expected; smoke emissions and emissions of unburned hydrocarbons (HC) and carbon monoxide (CO), which are generally found to be reduced for biodiesel; and the emissions of oxides of nitrogen (NO_x) which are expected to be increased at high load conditions compared to standard diesel fuels [3, 4]. Literature suggests that

these trends are due to the advances in injection timing, the shortening of ignition delay, advanced combustion phasing and increased flame temperatures associated with biodiesel usage [5, 6, 7, 8].

In relation to engine hardware compatibility, biodiesel is known to be miscible with fossil derived diesel and to have excellent lubricity and a high flash point [9]. However, there are concerns related to the decreased oxidative stability, degraded cold flow performance of the fuel [10], and of the deterioration of rubber fuel lines and seals due to the solvent properties of the biodiesel.

With the increased availability and use of biodiesels, it seems sensible to assess their compatibility with advanced diesel combustion modes—such as high-EGR low temperature combustion (LTC)—which are very likely to be integrated into diesel engine operating maps at selected load points in the short to medium term. It is hypothesised that the differentiating combustion characteristics of biodiesel fuels, which are strongly related to the presence of fuel bound oxygen, might help address some of the known challenges of high-EGR LTC—which include substantial oxygen-dilution and correspondingly increased ignition delays and emissions of HC and CO.

Previous studies [11, 12] support this hypothesis. The literature suggests that HC emissions in diesel LTC are due, predominantly, to over-lean, slow burning mixtures at low load [13, 14, 15], and under-mixed/richer mixtures at intermediate to high loads [16]. Petersen et al. [17] suggest that the reduction of HC emissions that is typically observed in low load LTC when operating with biodiesel is due to improvements in ignition quality (based on increased cetane number). Biodiesel fuels were reported to ex-

hibit shorter ignition delays, presumed to reduce mixture overleaning, and to exhibit faster premixed combustion durations (defined by Petersen as duration of 10-50 % mass fraction burned) leading to higher apparent (net) heat release rates (AHRR). The resulting advance in combustion phasing was thought to increase combustion temperatures and global reaction rates, thus enhancing HC and carbon monoxide (CO) oxidation (effects on thermal efficiency and NO_x emissions were not discussed, nor was the oxygen content of the biodiesels specified). The link between increasing biodiesel content and premixed burn rate at low-load has also been demonstrated in a study on late injection partially-premixed compression ignition (PPCI) LTC [18], although in this case the subsequent relationship between burn rate and HC was not observed—likely due to the constant combustion phasing strategy employed [19].

This study will consider the effects of an oxygenated FAME (Fatty Acid Methyl Ester) biodiesel on ignition, combustion and the emissions of HC and CO in both low-load and medium-load high-EGR LTC operating conditions—LTC in this work being defined by the authors as occurring when NO_x and smoke values are simultaneously near zero (here set at $<$20 ppm NO_x and $<$1 FSN smoke) regardless of dilution or combustion behaviour. Standard emissions and performance analyses as well as 'fast' hydrocarbon measurements for cycle resolved hydrocarbon sources will be used to understand the effect of increasing biodiesel concentrations on low temperature heat release and the subsequent high-temperature combustion processes and engine-out emissions.

2. Experimental methodology

2.1. Test cell and engine

Experiments were performed in a single-cylinder diesel engine research facility that is described in detail in a number of previous studies from the authors' research group [20, 21, 22, 23, 24]. The facility features an AVL 5402 single-cylinder research engine—a single cylinder version of typical 2.0 litre four-cylinder automotive high-speed direct injection (HSDI) diesel engine—mounted on a compact 38 kW dynamometer test bed. Table 1 details the engine and fuel system specifications. Fuelling parameters (injection pressure, timing, injected fuel mass) were fully and independently controllable using an ETAS INCA^{TM} engine controller. Oil and water conditioning to the engine was provided by an AVL 577 unit. An AVL 733 gravimetric fuel balance was used to measure fuel flow rate. Intake air charging was provided by a purpose-built stand-alone boost system consisting of a centrifugal supercharger, driven by an asynchronous AC motor with a variable frequency drive. For this application, the maximum mass flow rate of the compressor was limited to 0.05 kg/s with a maximum pressure ratio of 2.2:1. A boost pressure regulator maintained the desired flow rate into the engine, bypassing excess air to the atmosphere, thereby acting as a surge control mechanism for the supercharger. The system included closed loop PID controlled heating (1kW Farnam FT-200 charge air heater) and cooling (12kW air-water heat exchanger) systems enabling outlet air temperature control in the range 30 to 80°C independent of EGR rate. Further details of the boosting system design may be found in [25].

Figure 1 provides a schematic diagram of the facility's EGR system. The

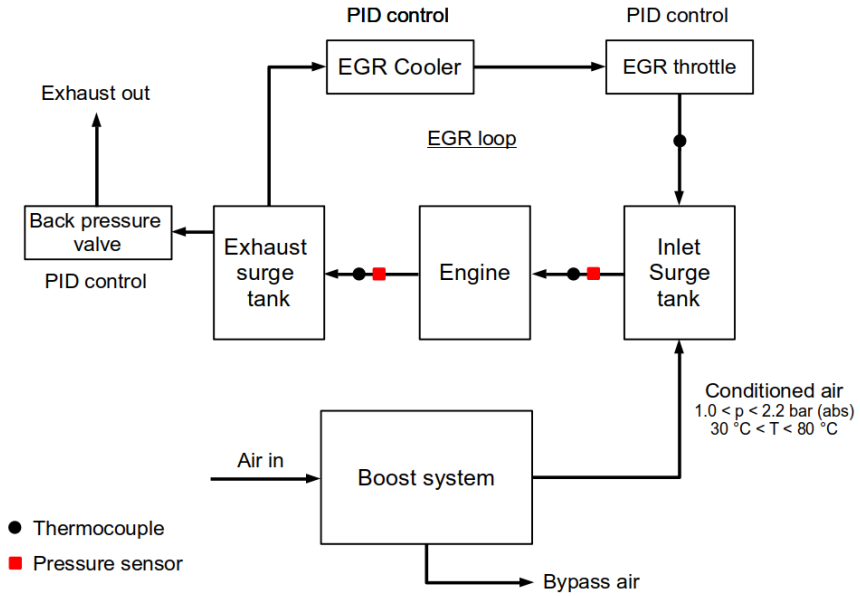

Figure 1: EGR loop and boost rig schematic

system provides control of the exhaust back pressure with an accuracy of ± 1% through an electronically actuated PID controlled butterfly valve in the exhaust line. The EGR rate to the engine was controlled with an accuracy of ± 0.5% by simultaneous adjustment of a PID controlled EGR throttle and the exhaust back pressure valve, where back pressure was maintained at 10-20 kPa above the inlet pressure in order to drive the EGR flow [25]. EGR temperature was controlled via PID control of coolant rate through the EGR cooler.

Engine out emissions of CO, CO_2, HC, and O_2 were measured by a HORIBA MEXA 7100HEGR. Intake manifold and in-cylinder pressures (respectively measured with a Kistler 4045A5 piezo-resistive transducer and a flush-mounted water cooled AVL QC34C transducer) were logged at a

Table 1: Engine and fuel injection system specifications

Property	Description
Engine	AVL 5402 Single Cylinder Diesel
Displaced volume	0.51 litre
Bore x Stroke	85 mm x 90 mm
Compression ratio	17.1:1
Rated Speed	4200 r/min
Maximum Power	16 kW
Nominal Swirl Ratio	1.78
Combustion Chamber	Re-entrant Bowl
Intake Ports	Tangential and Swirl
Injection System	Bosch Common Rail
Nozzle Type	Valve Covered Orifice (VCO)
Injector holes / Diameter	5 / 0.18 mm
Fuel injection pressure	90 MPa

resolution of 0.5 degree crank angle (°CA). This data was averaged over a minimum of 200 consecutive engine cycles and used to derive standard combustion parameters such as gross indicated mean effective pressure (GIMEP) and apparent heat release rate (AHRR). Emissions and flow rate measurements were logged at a frequency of 1 Hz over a duration of at least 2 minutes per test point.

2.2. Crank-angle aligned HC measurements

In order to obtain intra-cycle hydrocarbon emissions, a fast flame ionisation detector (Cambustion HFR 400 fast-FID), with a response time of

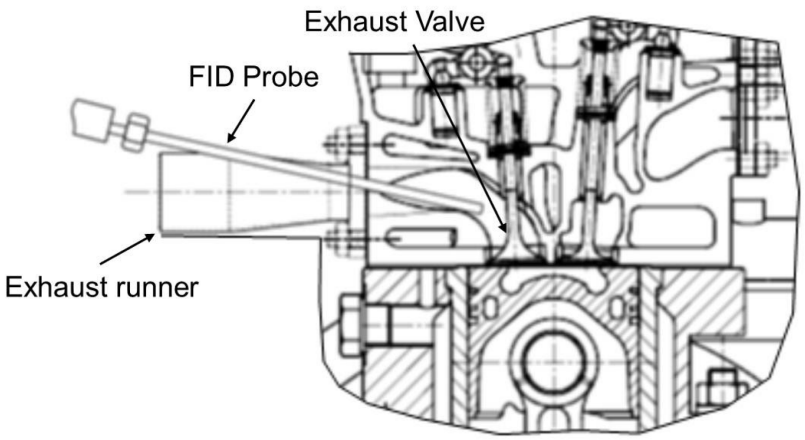

Figure 2: Cross-section though exhaust manifold and cylinder head detailing the positioning of the fast FID probe within the exhaust port with respect to the exhaust valve [26]

~1-2 ms, was positioned in the exhaust port 20 mm downstream of one of the two exhaust valves as shown in Figure 2 [26]. The raw fast-FID data was time-shifted in post-processing to account for the sample transit time and the instrument's response time to yield crank-angle aligned HC data [27].

2.3. Fuels and fuel properties

The properties of the base diesel and diesel/biodiesel fuel blends used in this investigation are shown in Table 2. The fuels are designated BXX, where XX represents the biodiesel content of the blend by percentage volume, i.e. B50 is 50 %v/v biodiesel. This investigation considers blends across the full range of available fuels, B0 is 'straight'petroleum-derived diesel, while B15 is a low-medium blend such as might be found commercially in the US and whose properties are goverened by ASTM D7467 [28]. B100 is a pure

biodiesel blendstock as specified by ASTM D6751 [29] while the B50 fuel that was used in this present work was blended specifically to investigate the space between the ASTM D7467 and D6751 regulations.

Vk40 is the kinematic viscosity of the fuel measured at 40°C. T90 is the 90 % distillation temperature of the fuel blend. The base diesel fuel was an automotive grade low sulphur diesel fuel (sulphur content < 10 mg/kg) compliant with current British Standard BS EN 590. The base fuel was a Fatty Acid Methyl Ester (FAME) biodiesel.

Table 2: Fuel properties

Property	Method	B0	B15	B50	B100
Density at 15°C ($kg.m^{-3}$)	DIN EN ISO 12185	833.6	840.3	858.0	883.6
Viscosity Vk40 ($mm^2.s^{-1}$)	DIN EN ISO 3104	2.81	2.97	3.50	4.53
Surface Tension ($mN.m^{-1}$)	ASTM D971	32.17	32.55	N/A	37.56
Lower heating value ($MJ.kg^{-1}$)	DIN 51900-3	42.89	41.62	40.34	37.34
C content (Wt%)		84.94	84.13	82.10	77.76
H content (Wt%)		15.05	14.45	12.90	12.56
O content (Wt%)		<0.03	1.42	4.84	9.68
Cetane number	DIN 51773	53.8	55.0	52.8*	61.2
T90 (°C)	DIN EN ISO 3405	330.4	336.5	341.1	N/A

* Note that the cetane number for the B50 fuel was supplied separately by a chemical analysis contractor which gave a variability of 52.8 $\pm$ 4.3. Despite the low value reported, the experimental results suggest a cetane number in-line with the increasing biodiesel content of the fuel.

2.4. Predicted effects of fuel properties

It is common practice to consider the ignition delay of an injected liquid fuel to be a function of two nominally independent components, the physical delay, τ_{phys} relating to the time necessary for the fuel and oxidant to form a locally combustible mixture, thus incorporating the effects of atomisation quality and volatility, and τ_{chem} relating to the kinetics of the chemical reaction [30, 31, 32], such that:

$$\tau_{\text{id}} = \tau_{\text{phys}} + \tau_{\text{chem}} \tag{1}$$

For a given engine and fuel injection system operating at the same stable operating point, both the physical and chemical delays will be dominated by the effects of fuel properties [32]. In this work a standard drop size correlation, eq. (2), previously developed by Elkotb [33] for a single hole plain orifice diesel injector was used to predict the effects of fuel composition on the atomisation quality as indicated by the Sauter Mean Diameter (SMD).

$$SMD = 6156\ \nu_L^{0.385}\left(\sigma\rho_L\right)^{0.737}\rho_g^{0.06}\Delta P_L^{-0.54} \qquad [\mu\text{m}] \tag{2}$$

where: *SMD* is the Sauter Mean Diameter, ν_L is the kinematic viscosity of the liquid fuel [$\text{m}^2.\text{s}^{-1}$], σ is its surface tension [N.m^{-1}], ρ_L is the fuel density [kg.m^{-3}], ρ_g is the density of the ambient gas [kg.m^{-3}] and ΔP_L is the pressure differential between the fuel rail and the ambient [bar]. A fuel temperature of 353 K was assumed for the calculations with 90 MPa fuel injection pressure and ambient conditions (air) at 800 K and 1.6 MPa. The values of fuel density and viscosity at 353 K were estimated from the values presented in Table 2 using, respectively, the relationship $\rho(T) = \rho(293) + 0.67 \times (293 - T)$

as suggested by fitting to the data of [34], and Vogel equations fitted to known data points. Surface tension values at 353 K were estimated using the relationship $\sigma(T) = \sigma(293) + 0.052 \times (293 - T)$ in general agreement with the trends observed by [35].

The Elkotb correlation predicts that the SMD of the injected fuel sprays will increase with increasing biodiesel content such that the predicted SMD of the B100 fuel is approximately 40 % greater than the B0 fuel (Figure 3). Although this level of percentage increase is within the range predicted by Ejim *et al.* [36], we note that it is substantially lower than the ∼100 % increase measured experimentally by Lee *et al.* [37] for a range of soybean and unpolished rice oil biodiesel blends and thus that it is possible that effects on SMD are underpredicted by the model. Nevertheless, the predicted trends are consistent with the literature: the greater the biodiesel content of the fuel the lower the atomisation quality. This reduced atomisation quality combined with the reduced mid-range fuel volatility typically associated with increasing levels of FAME biodiesel as shown in [38] is expected to increase the physical ignition delay, τ_{phys} with increasing levels of biodiesel.

With regards to the chemical delay, τ_{chem}, Yates and Viljoen [39] suggest a semi-empirical two-stage model, based upon Livengood and Wu's conservation of delay principle [40], such that

$$t_2 = t_1 + \tau_{h,CF}\left(1 - \frac{t_1}{\tau_{h,i}}\right) \tag{3}$$

where: t_2 is the overall ignition delay time, t_1 is defined by the appearance of the cool flame, and $\tau_{h,i}$ and $\tau_{h,CF}$ represent the characteristic ignition delays predicted by appropriate Arrhenius equations at the initial and post

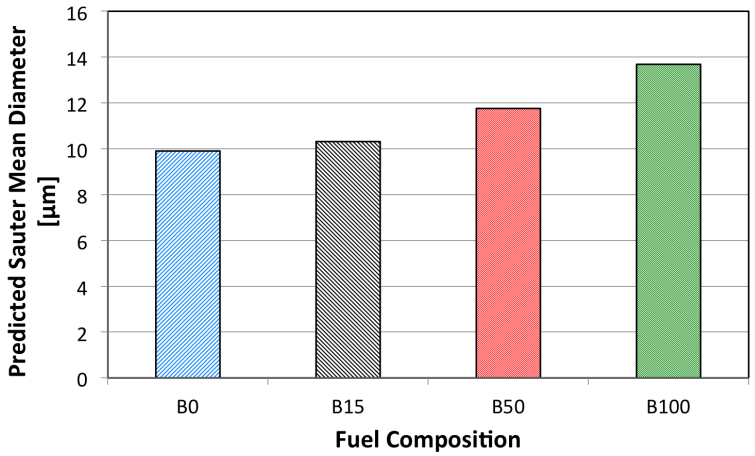

Figure 3: Variation of fuel spray SMD with fuel composition predicted by Elkotb correlation, eq. (2), assuming $\Delta P_L = 884$ bar, $\rho_g = 6.97$ kg.m^{-3}

cool flame conditions respectively. Yates and co-workers [39, 41] had earlier associated the low temperature pathway, the 'cool flame' delay and the 'NTC' delay, with the addition of molecular oxygen to an alkyl radical, $R^\bullet + O_2 \rightleftharpoons RO_2^\bullet$, followed by a second addition of O_2 after an internal H atom abstraction. High-temperature ignition (at temperatures $\sim$ 950 K) was said to be primarily driven by the decomposition of hydrogen peroxide, H_2O_2. Given the above, it seems reasonable to suppose that with all other factors held constant, the extra oxygen content associated with increasing levels of biodiesel should reduce the low temperature ignition delay and thus, through Equation (3), the overall chemical delay.

2.5. Engine test conditions

As detailed in Table 3, two engine speed/load points were considered: a medium-EGR dilution low-load point (3 bar GIMEP) and a high-EGR,

medium-load point (6 bar GIMEP)—both at a constant engine speed of 1500 rpm. Both of these test points were known from previous works to operate within the LTC regime. These points were chosen for further study due to their substantially different intake oxygen levels, 15.0% Y_{O2} vs 9.0% Y_{O2} respectively, which was thought to be significant in the context of oxygenated biodiesel combustion. It is important to note here that the symbol Y_{O2} is used within this study to denote the intake oxygen *mole* fraction. Engine fuelling for each load point was defined by operating the engine with standard B0 diesel at 0 % EGR. The resultant fuel energy input was then held constant across all fuels as indicated in the table of operating conditions and the intake oxygen mole fraction reduced to its target value through EGR dilution. Start of injection (SOI) timings were held constant for all fuels at each load point to ensure, as far as practically possible, similar fuel spray and thermal energy conditions during injection. The SOI timings chosen represent the MBT (minimum advance for best indicated torque) injection timings for the baseline B0 fuel. As noted from Table 2, the calorific value of the fuel decreases with increasing bio-diesel content. With respect to the variation of injection duration to maintain a constant energy input, the decrease in calorifc value is offset by the increased density of the biodiesel fuels such that the increase in injection duration going from B0 to B100 is < 0.5 °CA for the 3 bar GIEMP condition and < 0.6 °CA for the 6 bar GIMEP condition.

A stand-alone 10l gravity-feed fuel tank was employed to facilitate the changing of fuels between tests. The tank was connected to the single-cylinder engine fuel system via a flexible hose and in-line filter. At each

Table 3: Engine operating conditions

Parameter	Low load	Medium load
Engine speed (rpm)	1500	1500
GIMEP (bar)	3	6
Energy input (kJ/cycle)	0.35	0.72
Fuel injection pressure (MPa)	90	90
Fuel injection strategy	Single injection	Single injection
Start of injection (SOI)	-7.5 °CA ATDC	-30 °CA ATDC
Intake manifold pressure (kPa)	120	120
Intake manifold temperature (K)	329	345
Intake oxygen mole fraction	0.15	0.09
Coolant temperature (K)	353	353
Oil temperature (K)	363	363

fuel change the tank was emptied and cleaned, the in-line filter was replaced, and the low pressure side of the fuel system was flushed with 4l of the new fuel. Subsequently, the engine was warmed up and run on the new fuel for a minimum of one hour (at a fuel fuel mass flow rate ∼0.7 kg/hr in conventional diesel operating mode) in order to flush the high pressure system prior to switching to LTC for testing. The engine was then run for 15 minutes at LTC test point prior to data collection in order to stabilise fuel injection, boost system, EGR and back pressure parameters and achieve thermal equilibrium. In order to further resolve the intake oxygen concentration, which would typically vary ± 0.5% either side of the target value under the influence of the PID control, multiple data recordings were logged over the next 15 minute period. The data sets having the closest values to target value were then selected for analysis.

2.6. Data analysis and presentation

2.6.1. Combustion and heat release

AHRR was calculated from 200 cycle (minimum) mean data under all test conditions according to Equation (4) using a three point central differencing scheme for the numerical differentiation. Table 4, which follows the work of Cong et al. [42], defines the indicators that are used to characterise the low- and high-temperature ignition and heat release. Additionally, we take the 50% mass fraction burned crank angle (CA50) as an indicator of overall combustion phasing. Crank angle ranges for the pre-mixed and non-premixed phases of combustion vary with load point as indicated within the relevant discussions.

$$\mathrm{AHRR} = \frac{\gamma}{\gamma - 1} p \frac{\mathrm{d}V}{\mathrm{d}\theta} + \frac{1}{\gamma - 1} V \frac{\mathrm{d}p}{\mathrm{d}\theta} \tag{4}$$

where: p is the cylinder pressure, V is the cylinder volume, θ is the crank angle, and γ is the specific heat ratio – assumed to be constant at 1.39 as determined from the average gradient (across all four fuels) of the linear portions in both the compression and expansion strokes of the logarithmic plot of cylinder pressure vs cylinder volume for the lower load case. No significant deviation from this value, or trend in γ, was observed with changing fuel composition. A slightly lower value of γ, 1.37, was found for the higher load condition by the same procedure with again no significant variation or trend with fuel composition. However, accepting that both values are estimates, and that the error induced by inaccuracies in γ predominantly affect the magnitude of the AHHR as opposed to the timing of the derived combustion characteristics [43], γ=1.39 was applied to both load cases.

3. Results

3.1. Low load (1500 rpm, 3 bar GIMEP, 15.0% Y_{O2}, SOI = -7.5° CA ATDC)

Figure 4 shows the variation of AHRR with crank angle and increasing biodiesel content for the 3 bar GIMEP nominal, 15.0 % Y_{O2} operating point. Very similar AHRR behaviour is seen for all fuels. In all cases the AHRR data shows a clear low temperature heat release (LTHR) region followed by a rapid high temperature heat release (HTHR) phase corresponding to the combustion of the pre-mixed fraction of the charge. Note that, in contrast to

Table 4: Combustion and heat release parameter definitions

Parameter	Definition
SOL	Start of LTHR defined as the crank angle where the heat release rate is first positive (corresponding to the minimum value of the integrated heat release curve)
IDL	Ignition delay of the low temperature heat release defined as the duration from start of fuel injection (SOI) to SOL
DurL	Duration of the low temperature phase of combustion defined as the duration between SOL and the 5% mass fraction burned crank angle (CA5)
SOH	Start of the high temperature combustion defined as equal to CA5
IDH	Ignition delay to the start of HTHR defined by the interval SOH - SOI
DurH	High temperature combustion duration defined by the interval CA90 - CA5

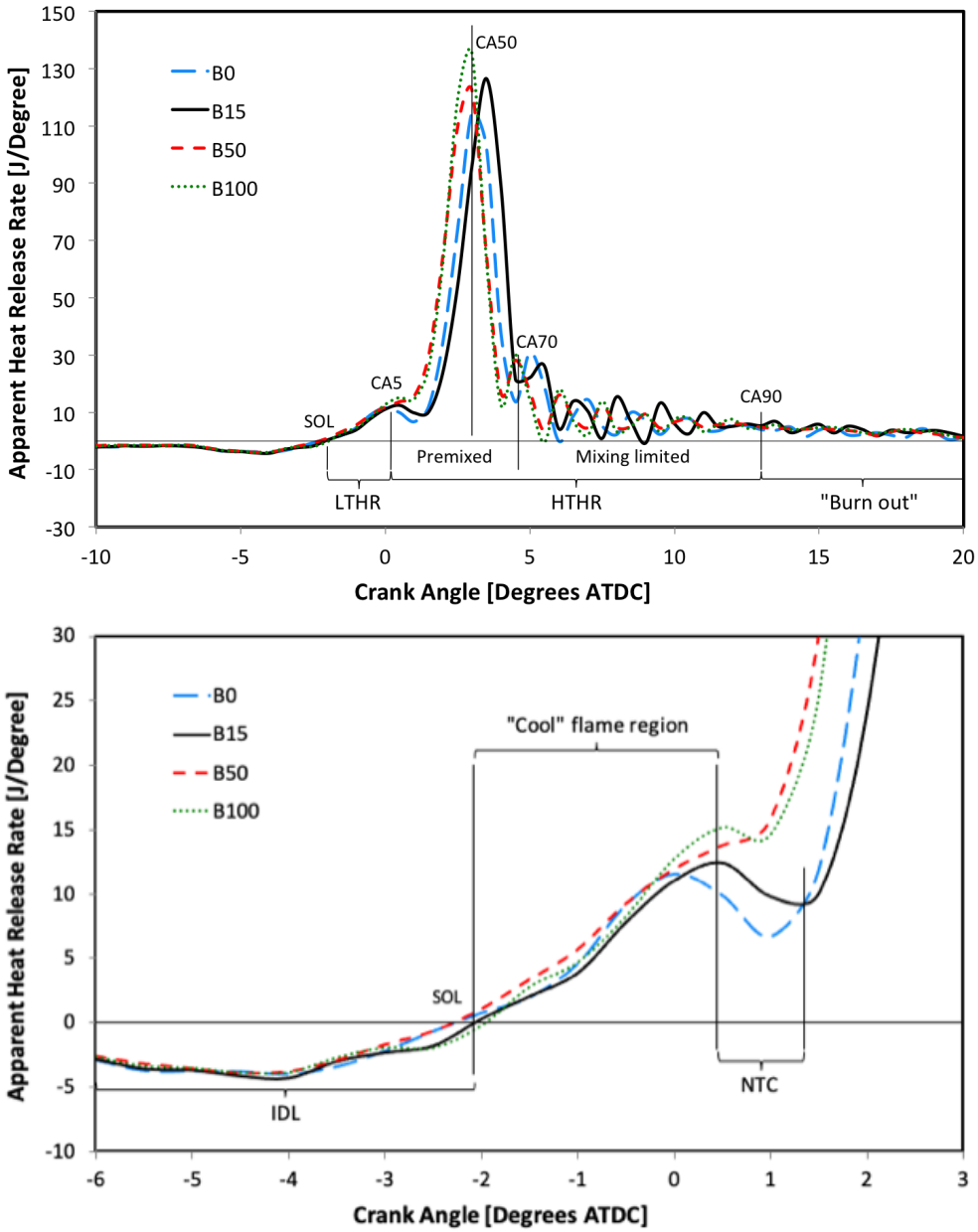

Figure 4: Variation of apparent (net) heat release rate with crank angle for the 3 bar GIMEP nominal, 15.0% Y_{O2}, SOI = -7.5 ATDC condition for B0, B15, B50 and B100 fuel blends, 200-cycle mean data (Upper image: HTHR and LTHR regions, lower image: detail of LTHR region).

convention, the pre-mixed phase is defined at this particular operating condition as the crank angle interval between 5 % and 70 % mass fraction burned, i.e., as shown in previous works [26], this is a substantially pre-mixed combustion condition. The pre-mixed phase is then followed by a significantly slower mixing-limited heat release phase as the in-cylinder charge begins to cool with expansion. The oscillatory heat release behaviour shown in the mixing-limited phase of combustion, which is characteristic of low to intermediate EGR rate diesel combustion [26], is attributed to the very high rate of pressure rise associated with pre-mixed combustion. These oscillations are not seen at high-EGR LTC conditions where the pressure rise rate is limited by oxygen availability [44]. The magnitudes and timings of the peak heat release rates are effectively constant within the precision of the experiment.

The lower graph of Figure 4, which details the LTHR phase of combustion, shows that the differing properties of the four biodiesel blends do not substantially change the LTHR phasing at this operating point. As shown in Figure 5, the ignition delay of low temperature heat release (IDL), and the duration of the LTHR (DurL) are also constant within the limits of the experimental error. Nonetheless, some differences are noted within the detail of the heat release traces with increasing levels of biodiesel addition. The LTHR can be split (in most cases) into a cool flame heat release and a negative temperature coefficient (NTC) region, in which the increasing temperature favours a decrease in the overall rate of reaction. Whereas the B0, B15, and B100 fuels exhibit distinct NTC regions, the B50 fuel does not. Peak LTHR values (assessed from the point of inflexion in the case of B50) are increased with increasing biodiesel content. Interestingly, this result is

consistent with the observations of Bunting et al. [45] who noted an increase in peak LTHR with increasing cetane number in HCCI combustion.

The results presented in Figure 5 show that the *net* effect of increasing the biodiesel content on ignition and combustion phasing at this low load, intermediate EGR condition is negligible (for constant injection timing). The increases in ignition delay that were expected as a result of the predicted decreases in atomisation quality and fuel volatility with increasing biodiesel content are not seen—suggesting that the fuel bound oxygen does in fact provide some form of compensating effect through reductions in the chemical delay term as previously suggested. There is an indication within the results plotted in Figure 5 that the peak heat release rate is slightly increased and advanced by the addition of increasing levels of biodiesel, although the observed changes are relatively minor at this operating point. It is thought that the increased oxygen content in the biodiesel reduces the amount of air entrainment and mixing required to attain locally flammable mixtures during the ignition delay period. An increase in the quantity of ignitable air-fuel mixture at the start of the HTHR would then increase the premixed heat release rate in a manner consistent with the presented results.

Figure 6 shows the variation of unburned hydrocarbon and CO emissions with biodiesel content for the 3 bar GIMEP nominal, 15.0 % Y_{O2} operating point. The results indicate that all of the biodiesel blends offer a HC and CO emissions advantage over conventional diesel fuel, with the maximum benefit seen for the B15 and B50 blends. It is well known that long ignition delays at low load LTC leads to increasing HC emissions from over-lean sources [15]. Colban *et al.* [46] have demonstrated the importance of reducing ignition

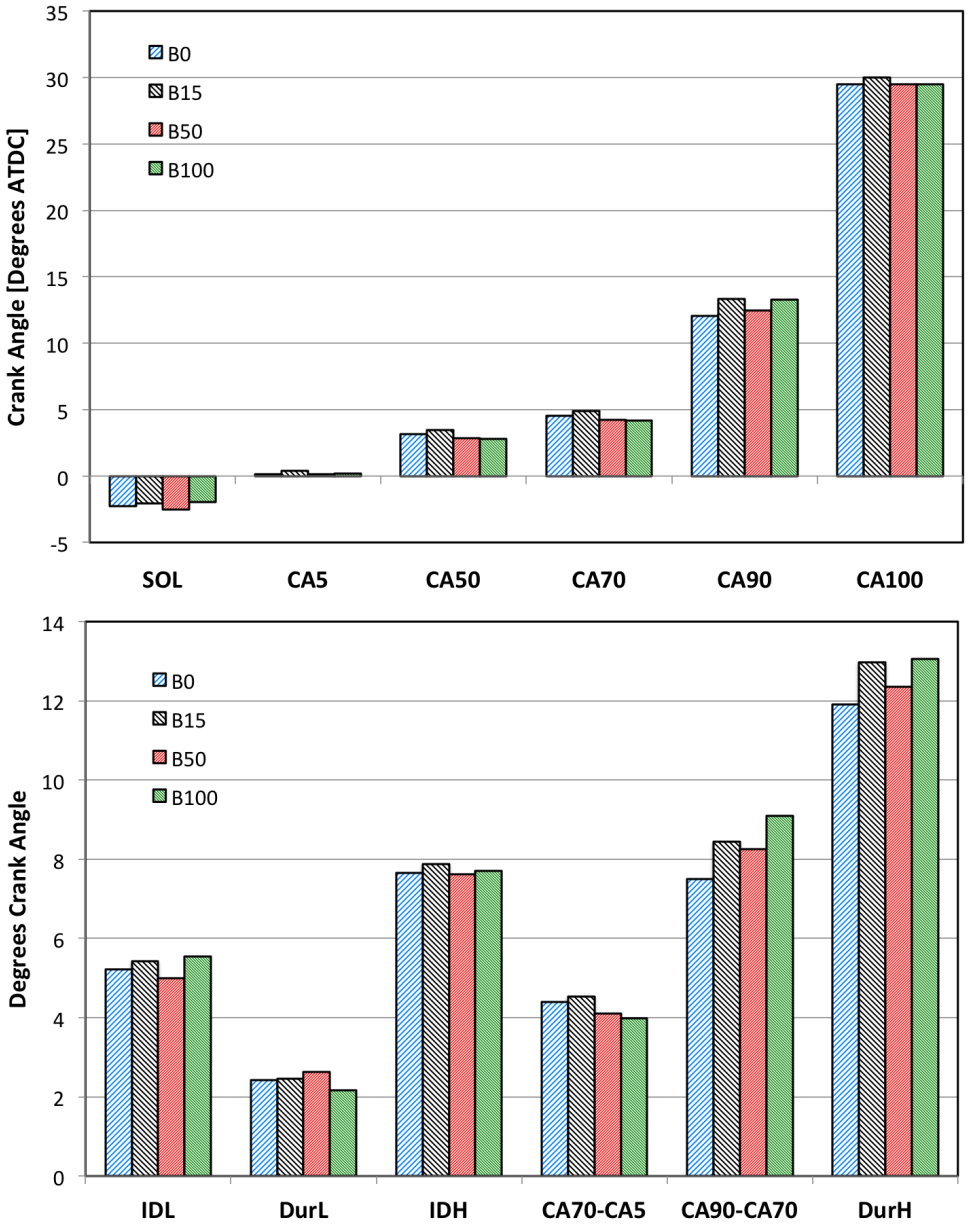

Figure 5: Cumulative heat release derived combustion metrics for the 3 bar GIMEP nominal, 15.0% Y_{O2}, SOI = -7.5 ATDC condition for B0, B15, B50 and B100 fuel blends (200 cycle mean data). Note that error bars are not shown on the data as the 95% confidence interval on all mean values < 0.1 degrees crank angle

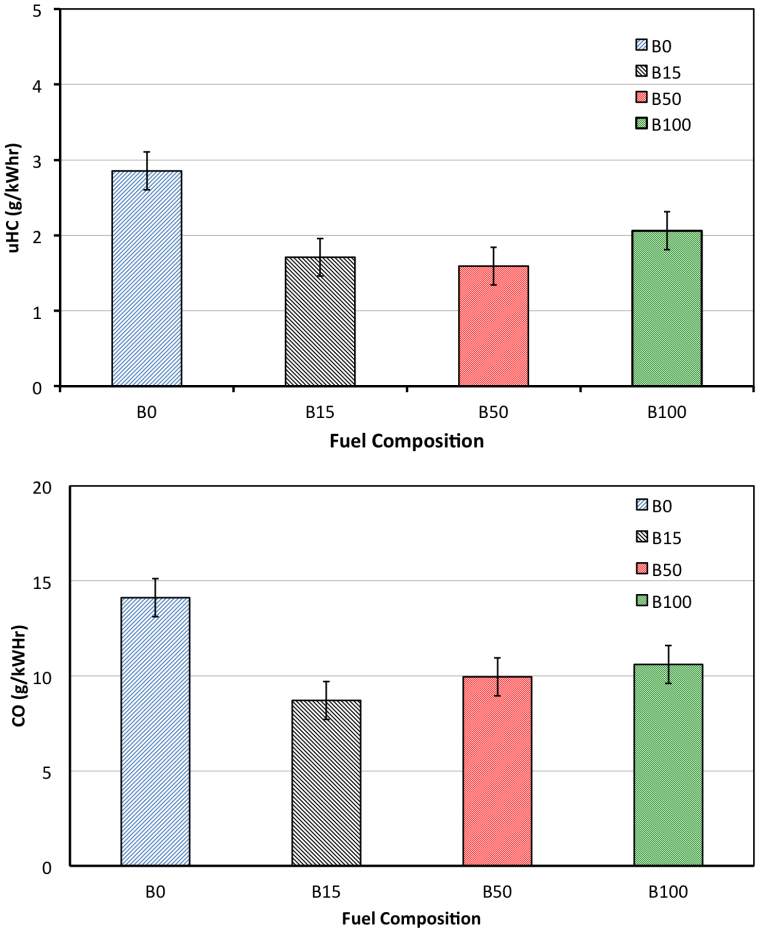

Figure 6: Variation of unburned hydrocarbon and CO emissions for the 3 bar GIMEP nominal, 15.0% Y_{O2}, SOI = -7.5 ATDC condition for B0, B15, B50 and B100 fuel blends.

delay at low loads in order to reduce these HC emissions. Given that the high and low temperature ignition delays are essentially constant for all fuels at this condition, it might be expected that the increased oxygen content of the biodiesel blends would serve to increase the number of over-lean regions within the cylinder—leading to higher HC emissions for the higher biodiesel blends. However, the authors' data does not reflect this expectation; at this load point all of the biodiesel blends show a reduction in HC and CO emissions compared to the base diesel. One possible explanation for these results is that the over-leaning potential of the fuel bound oxygen is mitigated by the reduced volatility of the biodiesel blends—thereby restricting the number of local mixture zones that exceed the lean flammability limit while still allowing for an overall increase in locally flammable regions with increasing biodiesel content at the start of HTHR as previously indicated by the increased premixed heat release rates.

3.2. Medium load (1500 rpm, 6 bar GIMEP, 9.0% Y_{O2}, SOI = -30° CA ATDC)

3.2.1. Combustion and heat release analysis

Figure 7 shows the variation of AHRR with crank angle and increasing biodiesel content for the 6 bar GIMEP condition. At this much lower oxygen concentration condition, increasing the biofuel content is seen to both increase the magnitude and advance the timing of the peak high-temperature heat release. The initial rate of change of the HTHR is also increased. Heat release for the LTHR as a percentage of the peak HRR value is low ($\sim$5%) and as a result it is not thought that the LTHR contributes significantly to HTHR behaviour—even though the LTHR is also advanced with increas-

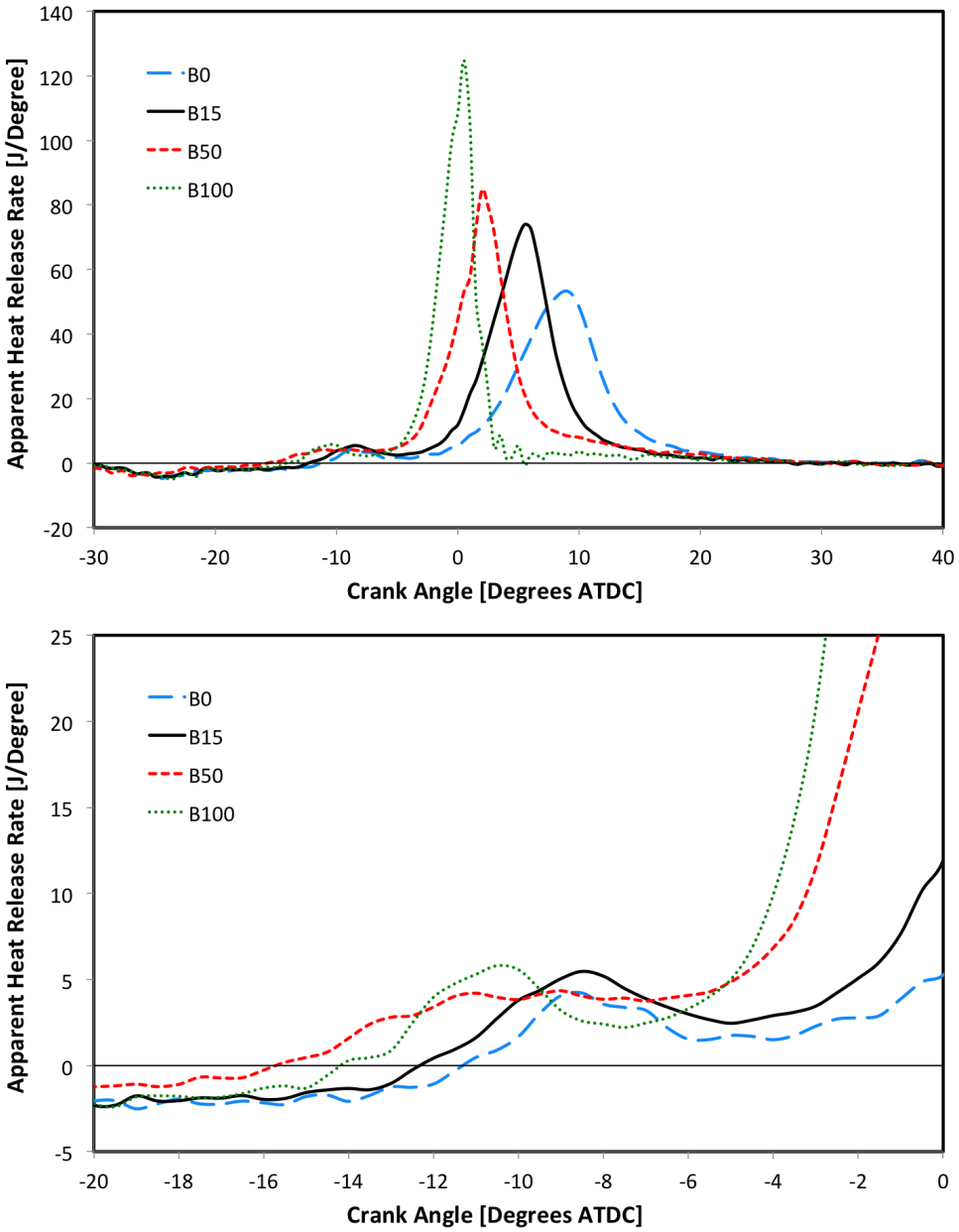

Figure 7: Variation of apparent (net) heat release rate with crank angle for the 6 bar GIMEP nominal, 9.0% Y_{O2}, SOI = -30 ATDC condition for B0, B15, B50 and B100 fuel blends, 200-cycle mean data (Upper image: HTHR and LTHR regions, lower image: detail of LTHR region).

ing biodiesel content (with the B50 and B100 fuels showing notably earlier LHTR than the B0 and B15 fuels) and the LTHR duration reduced as noted by Ickes *et al.* [18]. The cumulative heat release derived combustion metrics shown in Figure 8, clearly illustrate the advance in overall combustion phasing and the reduction in both low and high temperature ignition delays and combustion duration. These results are consistent with earlier works and are attributed to the increase in cetane number with increasing biodiesel content. Bunting *et al.* [45] have previously shown the advance of LTHR phasing with increased cetane number within the range $34 < \mathrm{CN} < 70$ (a range that encompasses the fuels used in this test). Peterson *et al.* [17] attributed observed changes in HTHR behaviour to the 'ignition quality' of the fuel, suggesting that the reduced ignition delays associated with higher cetane number fuels led to increased in-cylinder temperatures. It was postulated that these temperature increases would, in turn, increase premixed combustion rates by activating leaner mixtures into rapid combustion.

To further investigate this point, approximate bulk in-cylinder gas temperatures were calculated for the combustion of each fuel using the assumption of ideal gas behaviour and a constant value of volumetric efficiency. Figure 9 shows the resulting temporal evolution of bulk gas temperature for each fuel over the range of -30 to 60 degrees crank angle ATDC. The results indicate that the increase in the peak bulk gas temperatures between fuels is relatively modest, with the peak bulk gas temperatures of 1651 K for the B0 diesel fuel, 1717 K for the B15 blend, 1737 K for the B50 blend, and 1765 K for the B100 biodiesel.

It is clear that the low oxygen concentration and early injection timing

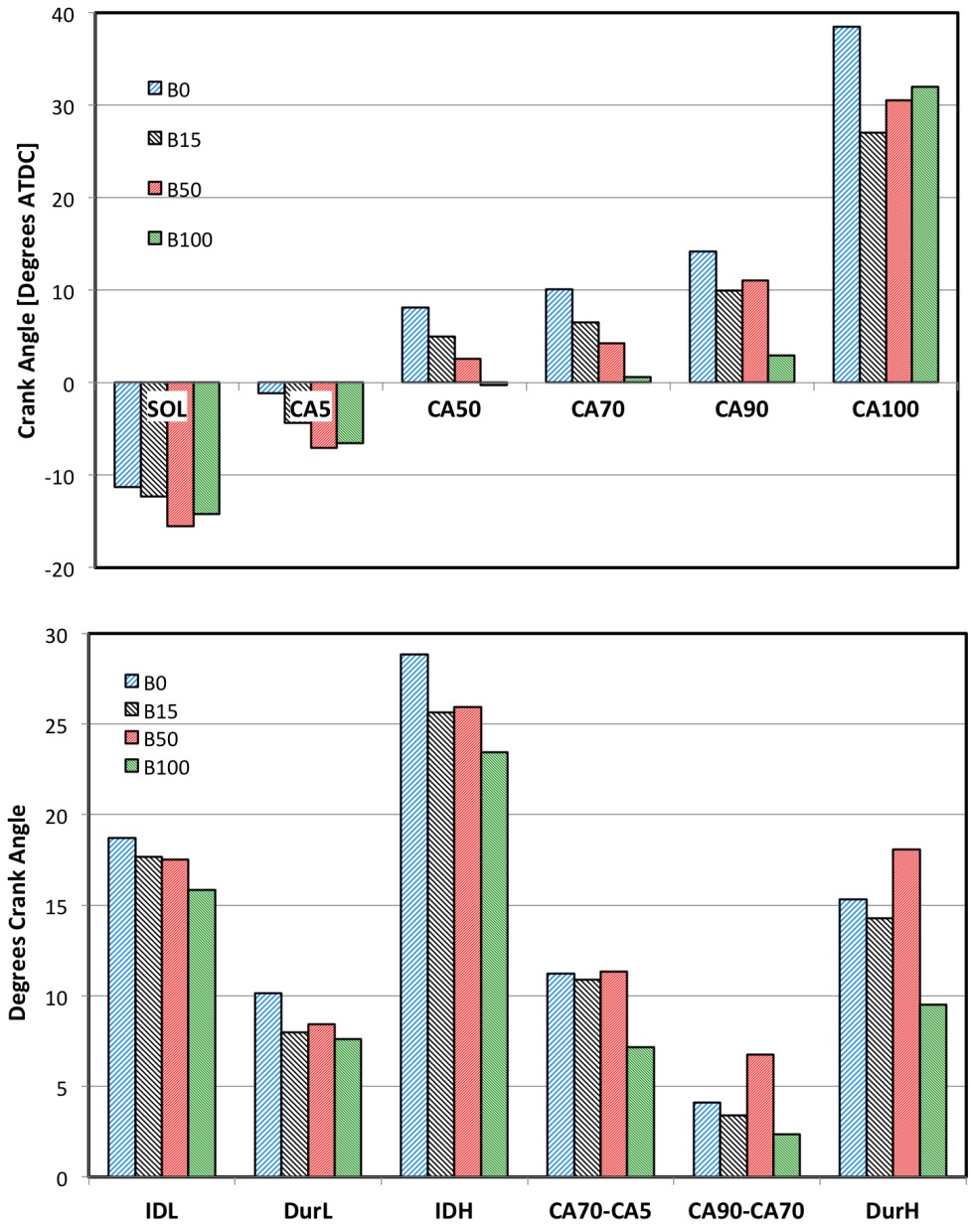

Figure 8: Cumulative heat release derived combustion metrics for the 6 bar GIMEP nominal, 9.0% Y_{O2}, SOI = -30 ATDC condition for B0, B15, B50 and B100 fuel blends (200 cycle mean data). Note that error bars are not shown on the data as the 95% confidence interval on all mean values < 0.1 degrees crank angle

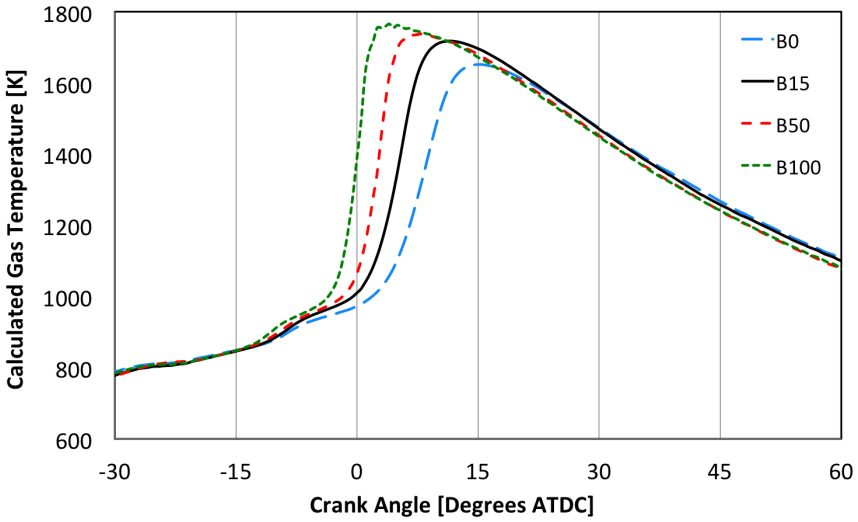

Figure 9: Calculated bulk gas temperature for the 6 bar GIMEP nominal, 9.0% Y_{O2}, SOI = -30.0 ATDC condition for B0, B15, B50 and B100 fuel blends (200 cycle mean data).

of this operating point leads to in-cylinder conditions which are less robust to the differences in the fuel properties than the earlier 3 bar, Y_{O2} = 15% condition. Low and high temperature combustion ignition delays (IDL and IDH) are extended from, respectively, about 5.5 °CA and 8 °CA at Y_{O2} = 15% to about 18 °CA and 25 °CA at Y_{O2} = 9%. In a previous study using an identical B0 fuel to that used in this work at a similar high-EGR LTC mid-load point, the authors demonstrated that increasing ignition delay and hence mixing time had the effect of reducing both the CO emissions and the HC emissions [20]. In the present work we observe that the ignition delay for both the low and high temperature heat release at this test point decreases with increasing biodiesel content, Figure 8, and that the HC emissions trends, Figure 10, are then in broad agreement with our previous results. It is accepted that the differences between the HC emissions of the

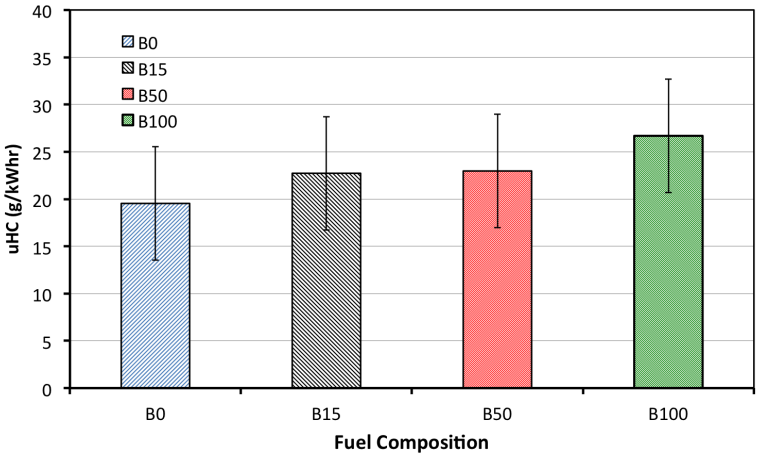

Figure 10: Variation of unburned hydrocarbon emissions for the 6 bar GIMEP nominal, 9.0% Y_{O2}, SOI = -30.0 ATDC condition for B0, B15, B50 and B100 fuel blends.

different fuel types shown in Figure 10 are not in themselves statistically significant; however, there is a clear trend in the results showing increasing HC emissions with increasing biodiesel content. Note that no CO emissions results are available from this point as, for all fuels, the CO emissions were above the measurement limit of the available analyser.

That the HC trends from the current work are consistent with our previous single fuel study in that the shorter the ignition delay the higher the HC emissions is interesting in light of the increased peak bulk gas temperatures for the higher biodiesel blends shown in Figure 9. Introducing the 'oxygen ratio' [19] in order to describe the proximity of each biofuel blend to its standard mixture stoichiometry, see Eqn.(5), it can be seen that effect of the fuel bound oxygen in the biodiesel blends is to shift the effective equivalence ratio of the fuel-oxidiser mixture towards a leaner global ratios compared to the corresponding oxygen equivalence ratio such that the B100 is the closest

to the stoichiometric condition followed by the B50, B15 and finally the B0 fuel (Figure 11). In contrast to the conventional 'equivalence ratio', which indicates stoichiometry based upon the amount of oxygen available in the oxidiser alone, or the 'oxygen equivalence ratio', which considers the oxygen in the oxidiser and in the recirculated exhaust gas, the oxygen ratio additionally considers the presence of oxygen in the fuel. The results also indicate that even accounting for the additional oxygen content of the biodiesel, the combustion conditions remain significantly 'rich' of stoichiometric, $0.8 <$ oxygen ratio < 0.9, for all of the tested blends fuels.

$$\text{Oxygen ratio} = \frac{A + B + C}{D} \tag{5}$$

where: $A =$ no. of moles of oxygen in the fuel, $B =$ no. of moles of oxygen in the oxidiser, $C =$ no. of moles of oxygen in the recirculated exhaust gas, and $D =$ no. of moles of oxygen required for stoichiometric combustion.

The present results would suggest that although the additional fuel bound oxygen associated with the higher biodiesel content fuels is able to influence positively the local autoignition process, advancing ignition and combustion (Figure 8), it is unable to mitigate for the resultant reduction in mixing time observed in a previous work [20]. Despite having greater oxygen availability, as evidenced by the oxygen ratio, and higher peak bulk temperatures, hydrocarbon emissions are higher for the higher biodiesel blends suggesting that under-mixed regions in the bulk gas remain a significant contributor to the HC emissions.

With regards to other potential sources of HC emissions and how these

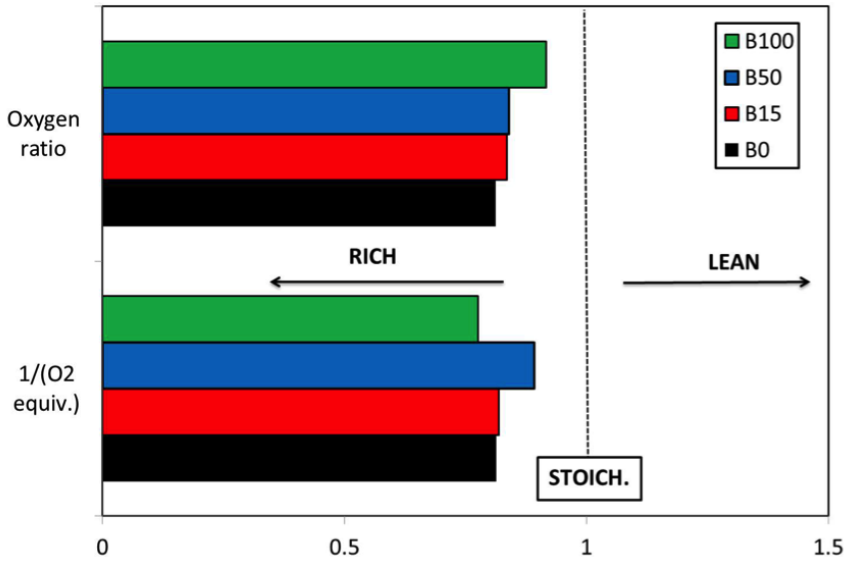

Figure 11: Oxygen ratio for 6 bar, 9.0% Y_{O2}, SOI = -30 ATDC condition for B0, B15, B50 and B100 fuel blends mixture compared to oxygen equivalence ratio

might be affected by fuel composition, the length of the ignition delay and the advanced injection timing of this test point suggest that there will be spray impingement on the piston bowl lip and within the bowl as observed by Sarangi *et al.* [24] and, as a result, piston wall films are expected. Note here that the literature regarding the effects of biodiesel content on spray penetration is relatively inconsistent with both increases and decreases in penetration length being reported [47, 48]. In all cases however, the reported changes are small at the injection pressures of the present work and thus, with respect to fuel impingement, the effect of advanced injection is likely to dominate. It may be argued that the lower volatility of the higher biodiesel blends would increase HC emissions from liquid films. However, it could also be argued that this negative effect would be mitigated by the increase in

Figure 12: Mean crank-angle aligned fast-FID data for 6 bar, 9.0% Y_{O2}, SOI = -30 ATDC condition for B0 (black line) and B15 (red line) fuel blends. Absolute values (ppm) adjusted to match cycle average emissions at EVO

in-cylinder temperature associated with the advanced combustion phasing of the lower volatility fuels as shown in Figure 9.

Further insight as to the sources of HC emissions and the effects of fuel composition may be obtained by consideration of the mean crank-angle aligned HC data presented in Figures 12, 13 and 14. Note here that it is the relative timing of HC emissions peaks between cycles that is of specific interest as opposed to the absolute HC values which have been adjusted to match the cycle averaged HC emissions for each particular fuel at the time of exhaust valve opening (EVO). For ease of analysis and discussion, the traces have been separated out into pairs.

Without instantaneous mass flow rate data, it is not possible to quan-

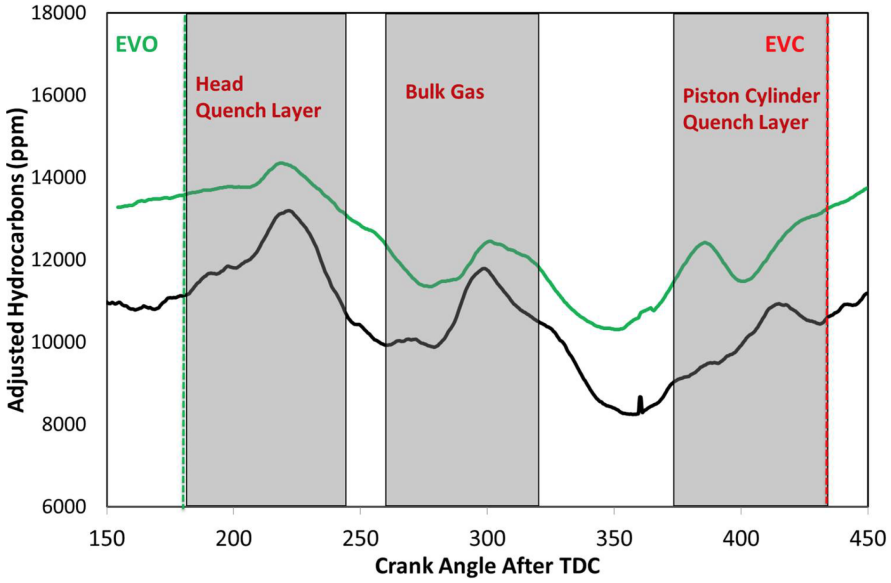

Figure 13: Mean crank-angle aligned fast-FID data for 6 bar, 9.0% Y_{O2}, SOI = -30 ATDC condition for B0 (black line) and B100 (green line) fuel blends. Absolute values (ppm) adjusted to match cycle average emissions at EVO

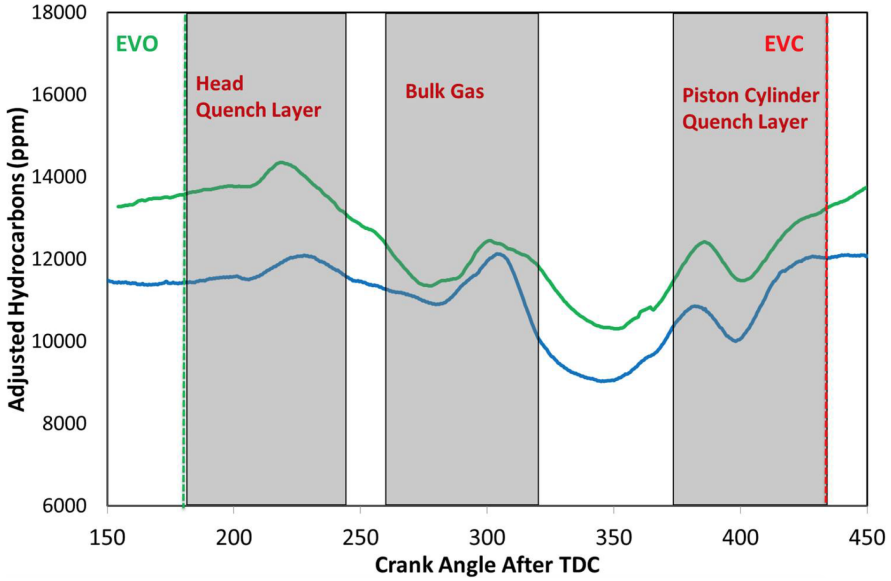

Figure 14: Mean crank-angle aligned fast-FID data for 6 bar, 9.0% Y_{O2}, SOI = -30 ATDC condition for B50 (blue line) and B100 (green line) fuel blends. Absolute values (ppm) adjusted to match cycle average emissions at EVO

tify the impact on cycle averaged emissions of the HC concentrations from different parts of the cylinder. Nevertheless, the results do show some interesting features with the most obvious differences between the cycle-resolved HC emissions of the different fuels observed between 375 and 430 degrees crank angle ATDC. Here, the 3rd FID signal peak is notably advanced for the B50 and B100 fuels compared to the B0 and B15 cases. According to Thompson *et al.* [49], HC emissions in this region represents the scrolled up HC from the piston wall crevices and the wall quench areas typically associated with spark ignited engines. Given the very early injection timing and the significant levels of premixing associated with the the current high EGR LTC strategy, and that this is a high-EGR operating point so that unlike a conventional diesel where the bulk gas is predominatly air the bulk gas will have some HC content, it is possible that the piston wall crevices and the wall quench areas are similarly the source of the observed HC emissions 'spike' in the results. It is thought that the advanced heat release of the B50 and B100 fuels (where a significant fraction of premixed burn occurs before TDC – Figure 8 refers) causes an earlier and greater compression of unburned fuel air mixtures into the squish region and piston crevices than for the B0 and B15 fuels. This piston crevice HC will be laid along the cylinder wall during the expansion stroke as described in [49]—being released earlier than for the B0 and B15 fuels cases due to its higher initial pressure. Further testing is required to confirm this hypothesis.

4. Conclusions

An experimental study was performed on a single-cylinder high-speed direct-injection diesel research engine to determine the effects of increasing biodiesel content on the combustion characteristics and HC emissions during high-EGR low tempertaure combustion operation. Two test points, a moderately dilute (15.0% Y_{O2}) 3 bar GIMEP/1500 rpm low-load condition and a very high-EGR (9.0% Y_{O2}) 6 bar GIMEP/1500 rpm medium-load condition, were examined.

The *net* effect of increasing the biodiesel content on ignition and combustion phasing at the low load, moderate dilution condition tested is negligible. Increases in ignition delay, which were expected as a result of predicted decreases in atomisation quality and fuel volatility with increasing biodiesel content were not seen, indicating that the increased fuel bound oxygen is able to provide a balancing effect through corresponding reductions in chemical delay.

Peak LTHR values for this condition are consistently increased with increasing levels of biodiesel as is the peak HTHR, which is also advanced – although the changes at low load are relatively minor. The changes in HTHR are attributed to the oxygen content of the biodiesel which is thought to reduce the amount of air entrainment and mixing required to attain locally flammable mixtures during the ignition delay period, thus increasing the volume of ignitable air-fuel mixture at the start of premixed combustion phase.

All of the biodiesel blends are shown to offer a HC and CO emissions advantage over conventional diesel fuel at low load, with the maximum benefit

seen for the B15 and B50 blends. However, the mechanism by which this benefit is obtained is not clear.

In contrast, at the much lower oxygen concentration condition medium load condition, increasing the biofuel content of the blend is seen to advance combustion phasing and reduce both the low and high temperature ignition delays and combustion duration. The magnitude and initial rate of change of the peak high-temperature heat release are also increased as are peak bulk temperatures. These results are consistent with earlier works in the literature and are attributed to the increased Cetane number of the higher biofuel content fuels.

HC emissions were found to increase with increasing biofuel content at this condition. The results suggest that the increased HC emissions are attributable to the advanced ignition timing. Mixing time, essential in this low oxygen availability environment, is decreased, while the earlier and greater peak pressure is thought to compress more bulk gas into the piston crevice regions. Note that, unlike in conventional diesel operation, the in-cylinder charge will contain a non-negligible amount of HC from previous cycles at this high-EGR LTC operating point, and that accordingly crevice volume HC emissions are similarly non-negligible.

CO emissions for all fuels at the medium load condition were above the measurement limit of the available analyser.

5. References

References

[1] European Union, Directive 2009/28/EC of the European Parliament and

of the Council of 23 April 2009 on the promotion of the use of energy from renewable sources and amending and subsequently repealing Directives 2001/77/EC and 2003/30/EC, Official Journal of the European Union 5 (2009) 2009.

[2] European Union, Directive (EU) 2018/2001 of the European Parliament and of the Council of 11 December 2018 on the promotion of the use of energy from renewable sources, Official Journal of the European Union 5 (2018) 82–209.

[3] M. Lapuerta, O. Armas, J. Rodriguez-Fernandez, Effect of biodiesel fuels on diesel engine emissions, Progress in Energy and Combustion Science 34 (2) (2008) 198–223.

[4] S. K. Hoekman, C. Robbins, Review of the effects of biodiesel on NOx emissions, Fuel Processing Technology 96 (2012) 237–249.

[5] A. Senatore, M. Cardone, V. Rocco, M. V. Prati, A comparative analysis of combustion process in DI diesel engine fueled with biodiesel and diesel fuel, SAE Technical Paper 2000-01-0691 (2000).

[6] W. F. Colban, P. C. Miles, S. Oh, On the cyclic variability and sources of unburned hydrocarbon emissions in low temperature diesel combustion systems, SAE Technical Paper 2007-01-1837 (2007). doi:10.4271/2007-01-1837.

[7] J. Sun, J. A. Caton, T. J. Jacobs, Oxides of nitrogen emissions from biodiesel-fuelled diesel engines, Progress in Energy and Combustion Science 36 (6) (2010) 677–695.

[8] C. J. Mueller, A. L. Boehman, G. C. Martin, An experimental investigation of the origin of increased NOx emissions when fueling a heavy-duty compression-ignition engine with soy biodiesel, SAE International Journal of Fuels and Lubricants 2 (2009) 789–816.

[9] G. Knothe, "Designer" biodiesel: optimizing fatty ester composition to improve fuel properties, Energy & Fuels 22 (2) (2008) 1358–1364.

[10] M. Andreae, H. Fang, K. Bhandary, Biodiesel and fuel dilution of engine oil, SAE Technical Paper 2007-01-4036 (2007).

[11] W. F. Northrop, S. V. Bohac, D. N. Assanis, Premixed low temperature combustion of biodiesel and blends in a high speed compression ignition engine, SAE International Journal of Fuels and Lubricants 2 (2009) 28–40.

[12] M. Zheng, M. C. Mulenga, G. T. Reader, M. Wang, D. S. Ting, J. Tjong, Biodiesel engine performance and emissions in low temperature combustion, Fuel 87 (6) (2008) 714–722.

[13] I. W. Ekoto, W. F. Colban, P. C. Miles, U. Aronsson, O. Andersson, S. W. Park, D. E. Foster, R. D. Reitz, UHC and CO emissions sources from a light-duty diesel engine undergoing late-injection low-temperature combustion, in: ASME 2009 Internal Combustion Engine Division Fall Technical Conference, American Society of Mechanical Engineers, 2009, pp. 163–172. doi:10.1115/icef2009-14030.

[14] M. P. Musculus, P. C. Miles, L. M. Pickett, Conceptual models for partially premixed low-temperature diesel combustion,

555 Progress in Energy and Combustion Science 39 (2) (2013) 246–283.
556 doi:10.1016/j.pecs.2012.09.001.

557 [15] M. P. Musculus, T. Lachaux, L. M. Pickett, C. A. Idicheria, End-
558 of-injection over-mixing and unburned hydrocarbon emissions in low-
559 temperature-combustion diesel engines, SAE Technical Paper 2007-01-
560 0907 (2007).

561 [16] T. Kitamura, T. Ito, Mixing-controlled, low temperature diesel combus-
562 tion with pressure modulated multiple-injection for HSDI diesel engine,
563 SAE International Journal of Engines 3 (2010) 461–478.

564 [17] B. R. Petersen, I. W. Ekoto, P. C. Miles, An investigation into the
565 effects of fuel properties and engine load on UHC and CO emissions
566 from a light-duty optical diesel engine operating in a partially premixed
567 combustion regime, SAE International Journal of Engines 3 (2010) 38–
568 55.

569 [18] A. Ickes, S. Bohac, D. Assanis, Effect of fuel cetane number on a pre-
570 mixed diesel combustion mode, International Journal of Engine Research
571 10 (4) (2009) 251–263.

572 [19] C. J. Mueller, M. Musculus, L. M. Pickett, W. J. Pitz, C. K. Westbrook,
573 The oxygen ratio: A fuel-independent measure of mixture stoichiome-
574 try, Tech. rep., Lawrence Livermore National Laboratory (LLNL), Liv-
575 ermore, CA (2003).

576 [20] O. Sogbesan, M. H. Davy, C. P. Garner, Insights into the hydrocarbon
577 and carbon monoxide emissions in moderately and highly dilute low

temperature combustion, Proceedings of the Institution of Mechanical Engineers, Part D: Journal of Automobile Engineering 228 (11) (2014) 1285–1296.

[21] O. M. Sogbesan, M. H. Davy, C. P. Garner, The potential of fuel metering control for optimising unburned hydrocarbon emissions in diesel low temperature combustion, SAE Technical Paper 2013-01-0894 (2013). doi:10.4271/2013-01-0894.

[22] A. K. Sarangi, C. P. Garner, G. P. McTaggart-Cowan, M. H. Davy, E. Wahab, M. Peckham, Load transient between conventional diesel operation and low-temperature combustion, Proceedings of the Institution of Mechanical Engineers, Part D: Journal of Automobile Engineering 229 (7) (2015) 850–865.

[23] A. K. Sarangi, C. P. Garner, G. P. McTaggart-Cowan, M. H. Davy, E. Wahab, M. Peckham, The effects of split injections on high exhaust gas recirculation low-temperature diesel engine combustion, International Journal of Engine Research 14 (1) (2013) 68–79. doi:10.1177/1468087412450987.

[24] A. K. Sarangi, C. P. Garner, G. P. McTaggart-Cowan, M. H. Davy, E. Wahab, M. S. Peckham, Effects of engine operating parameters on diesel low-temperature combustion with split fuel injection, Proceedings of the Institution of Mechanical Engineers, Part D: Journal of Automobile Engineering 226 (9) (2012) 1271–1286. doi:10.1177/0954407012440937.

[25] A. K. Sarangi, Diesel low temperature combustion: an experimental study, Ph.D. thesis, Department of Mechanical, Electrical, and Manufacturing Engineering, Loughborough University, UK (2012).

[26] O. Sogbesan, C. P. Garner, M. H. Davy, Effects of intake-port throttling on combustion behaviour in diesel low-temperature combustion, International Journal of Engine Research 19 (8) (2018) 827–838.

[27] S. Sogbesan, Strategies for reducing hydrocarbon emissions in diesel low temperature combustion, Ph.D. thesis, Department of Mechanical, Electrical, and Manufacturing Engineering, Loughborough University, UK (2016).

[28] ASTM, Standard specification for diesel fuel oil, biodiesel blend (B6 to B20) (2020).

[29] ASTM, Standard specification for biodiesel fuel blend stock (B100) for middle distillate fuels (2020). doi:10.1520/D6751.

[30] H. Bi, A. K. Agrawal, Study of autoignition of natural gas in diesel environments using computational fluid dynamics with detailed chemical kinetics, Combustion and flame 113 (3) (1998) 289–302.

[31] N. Wu, G. McTaggart-Cowan, W. Bushe, M. H. Davy, Effects of hydrogen addition on high-pressure nonpremixed natural gas combustion, Combustion Science and Technology 183 (1) (2010) 20–42.

[32] P. A. Caton, L. J. Hamilton, J. S. Cowart, Understanding ignition delay effects with pure component fuels in a single-cylinder diesel engine, Journal of Engineering for Gas Turbines and Power 133 (3) (2011) 032803.

[33] M. Elkotb, Fuel atomization for spray modelling, Progress in Energy and Combustion Science 8 (1) (1982) 61–91.

[34] B. Esteban, J.-R. Riba, G. Baquero, A. Rius, R. Puig, Temperature dependence of density and viscosity of vegetable oils, Biomass and bioenergy 42 (2012) 164–171.

[35] A. Chhetri, K. Watts, Surface tensions of petro-diesel, canola, jatropha and soapnut biodiesel fuels at elevated temperatures and pressures, Fuel 104 (2013) 704–710.

[36] C. Ejim, B. Fleck, A. Amirfazli, Analytical study for atomization of biodiesels and their blends in a typical injector: surface tension and viscosity effects, Fuel 86 (10) (2007) 1534–1544.

[37] C. S. Lee, S. W. Park, S. I. Kwon, An experimental study on the atomization and combustion characteristics of biodiesel-blended fuels, Energy & Fuels 19 (5) (2005) 2201–2208.

[38] P. Kattwinkel, C. Reith, M. Petersson, Different properties of biodiesel in comparison with standard diesel fuel and their impact on EURO VI exhaust aftertreatment systems, SAE Technical Paper 2012-01-1733 (2012).

[39] A. D. Yates, C. L. Viljoen, An improved empirical model for describing auto-ignition, SAE Technical Paper 2008-01-1629 (2008).

[40] J. Livengood, P. Wu, Correlation of autoignition phenomena in internal combustionengines and rapid compression machines, Proc. Combustion Institute 5 (1955) 347–356.

[41] A. D. Yates, C. L. Viljoen, A. Swarts, Understanding the relation between cetane number and combustion bomb ignition delay measurements, SAE International Journal of Fuels and Lubricants 113 (2004) 1510–1521.

[42] S. Cong, G. P. McTaggart-Cowan, C. P. Garner, E. Wahab, M. Peckham, Experimental investigation of low temperature diesel combustion processes, Combustion Science and Technology 183 (12) (2011) 1376–1400. doi:10.1080/00102202.2011.600740.

[43] G. Abbaszadehmosayebi, L. Ganippa, Determination of specific heat ratio and error analysis for engine heat release calculations, Applied Energy 122 (2014) 143–150. doi:https://doi.org/10.1016/j.apenergy.2014.01.028.

[44] S. Cong, An experimental study of low temperature combustion in a diesel engine, Ph.D. thesis, Mechanical, Electrical and Manufacturing Engineering, Loughborough University, UK (2010).

[45] B. Bunting, C. Wildman, J. Szybist, S. Lewis, J. Storey, Fuel chemistry and cetane effects on diesel homogeneous charge compression ignition performance, combustion, and emissions, International Journal of Engine Research 8 (1) (2007) 15–27.

[46] W. F. Colban, P. C. Miles, S. Oh, Effect of intake pressure on performance and emissions in an automotive diesel engine operating in low temperature combustion regimes, SAE Technical Paper 2007-01-4063 (2007).

[47] F. Millo, B. K. Debnath, T. Vlachos, C. Ciaravino, L. Postrioti, G. Buitoni, Effects of different biofuels blends on performance and emissions of an automotive diesel engine, Fuel 159 (2015) 614 – 627. doi:https://doi.org/10.1016/j.fuel.2015.06.096.

[48] P.-C. Chen, W.-C. Wang, W. L. Roberts, T. Fang, Spray and atomization of diesel fuel and its alternatives from a single-hole injector using a common rail fuel injection system, Fuel 103 (2013) 850 – 861. doi:https://doi.org/10.1016/j.fuel.2012.08.013.

[49] N. D. Thompson, J. S. Wallace, Effect of engine operating variables and piston and ring parameters on crevice hydrocarbon emissions, SAE International Journal of Engines 103 (1994) 718–736.